

REPORT DOCUMENTATION PAGEForm Approved
OMB No. 074-0188

Public reporting burden for this collection of information is estimated to average 1 hour per response, including the time for reviewing instructions, searching existing data sources, gathering and maintaining the data needed, and completing and reviewing this collection of information. Send comments regarding this burden estimate or any other aspect of this collection of information, including suggestions for reducing this burden to Washington Headquarters Services, Directorate for Information Operations and Reports, 1215 Jefferson Davis Highway, Suite 1204, Arlington, VA 22202-4302, and to the Office of Management and Budget, Paperwork Reduction Project (0704-0188), Washington, DC 20503

1. AGENCY USE ONLY (Leave blank)		2. REPORT DATE 9/9/99	3. REPORT TYPE AND DATES COVERED Final Tech. Report 2/1/91-5/31/99	
4. TITLE AND SUBTITLE Some Novel In Situ Studies of Strained Semiconductor Epitaxy on Patterned/Compliant Substrates			5. FUNDING NUMBERS Contract/Grant number: N00014-91-J-1464	
6. AUTHOR(S) Professor Anupam Madhukar				
7. PERFORMING ORGANIZATION NAME(S) AND ADDRESS(ES) University of Southern California Dept. of Materials Science & Engineering 3651 Watt Way, VHE 506 Los Angeles, CA 90089-0241			8. PERFORMING ORGANIZATION REPORT NUMBER	
9. SPONSORING / MONITORING AGENCY NAME(S) AND ADDRESS(ES) Office of Naval Research Electronics Division 800 North Quincy St. Arlington, VA 22217-5660			10. SPONSORING / MONITORING AGENCY REPORT NUMBER	
11. SUPPLEMENTARY NOTES N/A				
12a. DISTRIBUTION / AVAILABILITY STATEMENT Approved for public release; distribution unlimited				12b. DISTRIBUTION CODE
13. ABSTRACT (Maximum 200 Words) This final technical report summarizes the most important findings of the research work on (a) growth and properties of highly lattice mismatched InAs on GaAs(001) planar and patterned substrates and (b) growth of lattice matched GaAs/AlGaAs and of low lattice mismatch InGaAs/AlGaAs on patterned GaAs for, respectively, the creation of nanostructures and reduction of misfit dislocations. The specific accomplishments include the demonstration of (1) the quantum box nature of the 3D epitaxial InAs islands via photoluminescence excitation spectroscopy, (2) vertically self-organized growth of the island quantum dots, (3) control on island quantum dot size, density, and shape, (4) spatially-selective growth of quantum wires and boxes via size-reducing growth on mesas, (5) reduction of misfit dislocation in films on submicron and nanometer scale mesas, and (6) the nature of atomic level stress in strained Ge islands on planar Si(001) and in Ge overlayers on Si(001) mesas as obtained from multimillion atom classical molecular dynamics.				
14. SUBJECT TERMS Quantum wires and dots, strained epitaxy, molecular beam epitaxy, atomic force/scanning tunneling microscopy, transmission electron microscopy, photoluminescence, quantum dot laser, misfit dislocation, molecular dynamics, Ge island, Si mesas.				15. NUMBER OF PAGES
				16. PRICE CODE
17. SECURITY CLASSIFICATION OF REPORT UNCLASSIFIED	18. SECURITY CLASSIFICATION OF THIS PAGE UNCLASSIFIED	19. SECURITY CLASSIFICATION OF ABSTRACT UNCLASSIFIED	20. LIMITATION OF ABSTRACT	

FINAL TECHNICAL REPORT

**Contract No. N00014-91-J-1464
(February 1, 1991 - May 31, 1999)**

**Some Novel In Situ Studies of Strained Semiconductor Epitaxy on
Patterned/Compliant Substrates**

P.I.: Anupam Madhukar

August 1999

**Submitted to
Dr. Larry Cooper
Electronics Division
Office of Naval Research
800 North Quincy Sr.
Arlington, VA 22217-5660**

**by
University of Southern California
Department of Materials Science & Engineering
Los Angeles, CA 90089-0241**

DTIC QUALITY INSPECTED 4

19991019 034

Table of Contents

I.	Statement of the Problems Examined.....	3
II.	Summary of the Most Important Results.....	4
II.1	Highly Strained Epitaxy on Planar Substrates: 3D Island Quantum Dots.....	4
II.1.a	In-situ UHV STM/AFM studies of InAs 3D island evolution and implications for an atomistic kinetic framework	4
II.1.b	Re-entrant behaviour of 2D-3D morphology change	6
II.1.c	Simulations of atomic-scale stress distribution in coherent 3D island systems	7
II.1.d	Island induced stress in capping layer and Vertically Self-Organized quantum dots.....	11
II.1.e	Independent manipulation of SAQD Density, Size and Shape: The Variable Deposition Amount (VDA) Structures	15
II.2	Unstrained and Strained Growth on Patterned Mesas: Size-Reducing Growth, Defect Reduction, and Spatially Selective Quantum Dot Growth	19
II.2.a	GaAs/AlGaAs Quantum Wires and Boxes via Growth on Mesas	20
II.2.b	Misfit Dislocation Reduction at low misfits via growth on mesas.....	21
II.2.c	Strain Accomodated Quantum Boxes on Nanoscale Square Mesas	22
II.2.d	Spatially-Selective InAs SAQDs via Growth on Nanoscale Width Stripe Mesas	27
III.	List of Publications.....	29
IV.	List of Personnel Supported.....	33

I. Statement of the Problems Examined

Efforts under the above referenced grant were focused upon a combined experimental and computer simulation examination of the atomistic nature of lattice matched and mismatched (i.e. strained) semiconductor epitaxy on planar and patterned substrates with a view to the realization of high quality quantum wells, wires, and boxes. The following issues were of particular focus:

- (1) The nature of lattice matched (GaAs/AlGaAs) growth on non-planar patterned substrates for the creation of growth-controlled nanostructures (quantum wires and boxes).
- (2) The nature of low lattice mismatch ($\text{In}_x\text{Ga}_{1-x}\text{As}/\text{GaAs}$, $x < 0.25$) strained epitaxy on planar and patterned substrates for misfit dislocation reduction.
- (3) The nature of the evolution of three-dimensional (3D) defect-free (i.e. coherent) islands in highly strained epitaxy, such as InAs on GaAs(001) and Ge on Si(001), and the nature of atomic scale stress/strain spatial distribution in such 3D island quantum dots dubbed self-assembled epitaxial quantum dots (SAQDs).
- (4) Innovative ways of controlling the density, size, shape, and spatial arrangement of the SAQDs.
- (5) The nature of highly strained epitaxy on nanoscale mesas and spatially inhomogeneous synergistic stress/strain distribution between the overlayer and the compliant nature of the mesas.

Towards these objectives, a combination of the following approaches were employed.

1. Solid source molecular beam epitaxy of AlGaAs/GaAs(001) and InGaAs/GaAs(001) systems on planar and patterned substrates.
2. Transmission electron microscope studies of the GaAs growth profile evolution on stripe and square mesas as revealed through periodic placement of AlGaAs marker layers.

3. Transmission electron microscope studies of misfit dislocation reduction in the growth of $\text{In}_x\text{Ga}_{1-x}\text{As}$, $x < 0.25$ (i.e. $< 2\%$ strain) on submicron width stripe mesas.
4. In-situ, i.e. all ultra-high vacuum (UHV) transfer, and ex-situ (i.e. ambient) atomic force microscope (AFM) and scanning tunneling microscope (STM) studies of the nature of the morphological evolution of the InAs surface, the formation of the 3D islands, and their density, size, and shape evolution as a function of the deposited material amount.
5. Transmission electron microscope studies of the structural nature of the 3D island quantum dots and of InAs overlayers on in-situ prepared (via size-reducing epitaxy) nanoscale GaAs square mesas.
6. Photoluminescence (PL) and PL excitation (PLE) studies of the grown quantum box structures.
7. Cathodoluminescence studies of the quantum wire and quantum box structures.
8. Large scale (greater than million atom) classical molecular dynamics simulations of the nature of the atomic scale spatially inhomogeneous stress and strain distribution in 3D pyramidal island quantum dots on planar substrates and of flat morphology overlayer quantum boxes on nanoscale mesas. The Ge/Si(001) combination was used for the simulations in view of the well-tested nature of the Stillinger-Weber interatomic potentials for Ge and Si available in the literature.

In the following we provide a brief summary of the most important results obtained. Details are found in the publications referred to from the list provided in section III.

II. Summary of the Most Important Results

II.1 Highly Strained Epitaxy on Planar Substrates: 3D Island Quantum Dots

(a) In-Situ UHV STM/AFM studies of InAs 3D island evolution and implications for an atomistic kinetic framework:

The UHV interconnected MBE growth and STM/AFM characterization chambers in our unique all UHV interconnected six-chamber growth, processing, and characterization system enabled careful and systematic examination of the nature and

process of 3D island evolution as a function of InAs coverage on GaAs(001). The experimental findings are detailed in publication nos. 43, 44, and 45.

Briefly, our studies revealed the presence, during the 2D to 3D morphology evolution, of a varying mass transfer between structural features that could be unambiguously identified as 2D (i.e. 1 monolayer high), quasi-3D (between 2ML and 4ML high), and 3D (≥ 5 ML in height). The evolution of the density of these different structural features at 500°C as a function of InAs deposition amount Θ is summarized in fig. 1. The quasi-3D clusters (between 2ML and 4ML high), labeled Q3D clusters in the middle

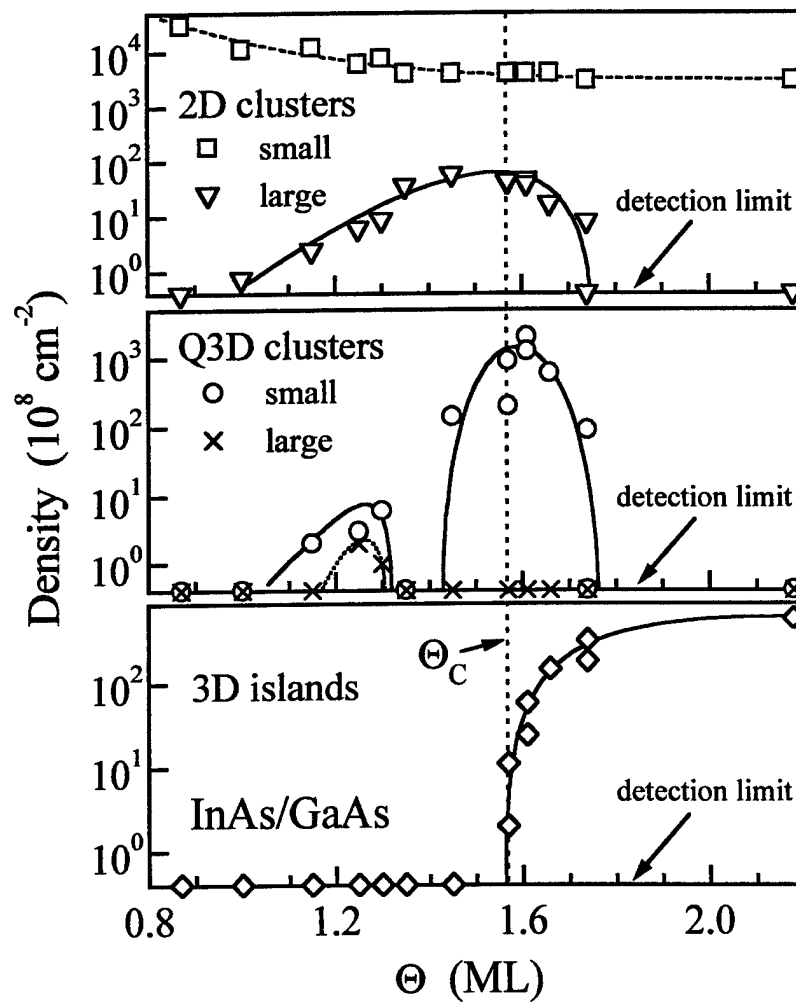


fig. 1

panel, are broken into small (< 30 nm base size) and large (> 30 nm base size, but typically > 50 nm). These Q3D clusters are found to mediate the 2D to 3D morphology change and

to play an important role in the mass re-distribution on the surface. These results provide clear evidence of local (and hence globally inhomogeneous) strain and surface/interface energy in determining the evolving relative quantitative significance of surface kinetic process during 3D island formation and subsequent evolution.

(b) Re-entrant behavior of 2D-3D morphology change:

The coherent nature of the 3D islands caused explosive growth in the examination of their optical behavior as quantum boxes by groups around the globe and of their potential for quantum box based injection lasers by a few, including us. Reliable interpretations of the origin of optical emission and lasing demanded that careful and systematic combined atomic level structural and optical studies be carried out on comparable samples in order to understand the atomistic mechanism of strain-induced evolution of structural features and their role in the optical response. We undertook this challenging task under the support of this grant. A remarkable discovery of a re-entrant behavior, as described below, was made and reported in a paper published in Phys. Rev. Lett. (publication no. 42).

Briefly, InAs structural features up to five monolayers high appear at $\sim 1.25\text{ML}$ deposition of InAs, disappear, and reappear prior to the onset of well-developed 3D islands at 1.57ML , thus manifesting a hitherto unrecognized reentrant behavior in the formation of 3D islands (see middle panel of fig. 1). The optical signature of this reentrant behavior is shown in fig. 2. The narrow peak near 8500\AA , which evolves with increasing InAs deposition and vanishes just beyond Θ_c at 1.57ML , is attributed to the recombination in the wetting layer (WL). The almost Gaussian peak observed at 10200\AA for the 2.00ML sample is attributed to recombination in 3D island quantum dots (QDs). A careful analysis of the PL spectra of the 1.15ML and 1.25ML samples reveals for the first time peaks at 9380\AA and 9733\AA , respectively, in addition to the WL emission. By contrast, no PL in the 9200\AA to 10300\AA region could be resolved for the 1.35ML and 1.45ML samples. And then, at 1.55ML deposition (just below Θ_c) PL reappears in this spectral region and finally develops into 3D island PL, thus establishing a re-entrant PL behavior paralleling that of the 3D structural features seen in the STM studies. These results provide new insights into

the long-standing problem of the kinetic aspects of 2D to 3D morphology change not embodied in the widely encountered Stranski-Krastanow growth mode. Moreover, this systematic study unambiguously identified the origin of the lasing in our InAs quantum box-based laser structures as arising from the 3D island quantum boxes and not from other structural features (see point d). The spectral position of the observed lasing line (see point d) is shown as a dashed straight line in fig. 2 for later reference. Since the laser structures contain InAs layer(s) with 2ML InAs deposition for which the quasi 3D clusters have vanished, the origin of lasing is attributed to the well formed, coherent InAs islands.

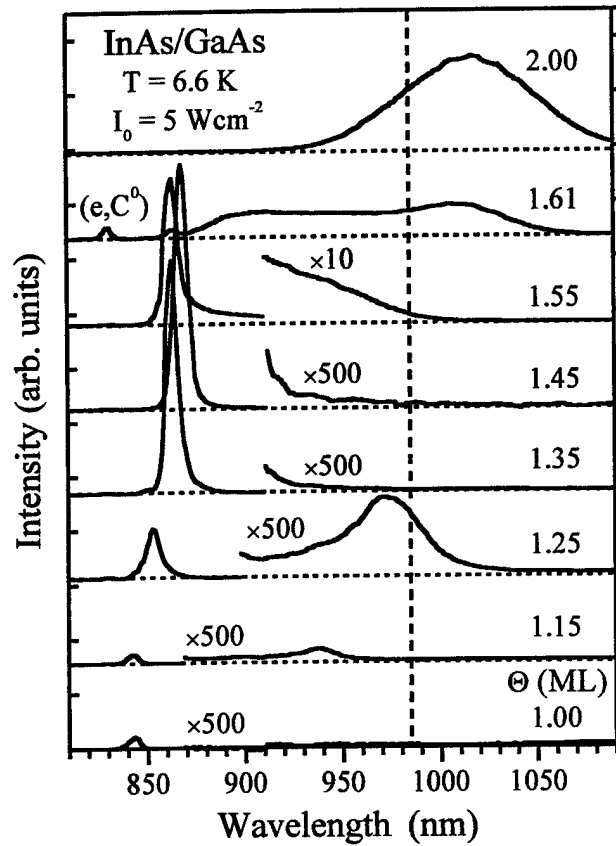


fig. 2

(c) *Simulations of atomic-scale stress distribution in coherent 3D island systems:*

Multimillion particle classical molecular dynamics simulations on parallel computing platforms were undertaken utilizing the Ge/Si(001) combination as a model vehicle represented by Stillinger-Weber interatomic potentials. Details may be found in

publication nos. 40, 41, and 49. Briefly, typical number of atoms in the simulation cell are $\sim 1.5 \times 10^6$ and the conjugate gradient energy minimization is employed to obtain locally stable configuration such that the net force on each atom is less than 10^{-4} eV/Å. Energies, strains, and stresses are calculated for such atomic configurations. The atomic level stress components are calculated utilizing the following expression:

$$\sigma_{\alpha\beta} = -\frac{1}{\Omega_0} \left[\frac{p_i^\alpha p_i^\beta}{m_i} + \frac{1}{4} \sum_j \left(\gamma_{ij}^\beta f_{ij}^\alpha + \gamma_{ij}^\alpha f_{ij}^\beta \right) \right]$$

in which $(\alpha, \beta) = (x, y, z)$, m_i and \vec{p}_i are the mass and momentum of atom i , \vec{r}_{ij} is the distance from atom i to j , \vec{f}_{ij} is the force on atom i due to j , and Ω_0 is the average atomic volume.

In fig. 3 is shown the Ge 3D island energy as a function of the number of Ge atoms (N) in $\langle 100 \rangle$ oriented square base islands with $\{105\}$ sidewalls. The shape and geometry is as reported in the STM studies in the literature. The island energy, $E(N)$, is defined as,

$$E(N) = E(\text{WL}+3\text{D}) - E(\text{WL}) - N \cdot \epsilon_{\text{Ge}}$$

in which $E(\text{WL}+3\text{D})$ is the energy of the relaxed state of the 3D island with $\{105\}$ sidewalls atoms rebonded sitting on a 3ML thick Ge wetting layer (WL) having a (2×1) reconstruction on the Si(001) substrate, $E(\text{WL})$ is the energy of a system with no island but only the planar 3ML thick Ge (2×1) wetting layer relaxed to its own lowest energy state, and ϵ_{Ge} is the cohesive energy per atom of the bulk Stillinger-Weber Ge. Note that the island energy so defined includes all the energy changes of the Si atoms in the substrate and in the Ge WL. The dashed line in fig. 3 is a fit of the form

$$E(N) = (aN^{2/3} + bN + c) = (a'V^{2/3} + b'V + c)$$

in which $V = (N \cdot a_{\text{Ge}}^3 / 8)$ where $a_{\text{Ge}} = 5.659 \text{ Å}$ is the bulk Ge lattice constant. The fitted values of a' and b' are found to be $a' = 26.6 \text{ meV/Å}^2$ and $b' = 1.36 \text{ meV/Å}^3$. The fitted functional form provides the basis for the widespread practice of representing island energy as the sum of volume-like and surface-like terms. The numerical values of the coefficients, when compared to those that would be calculated using numerical values of

the bulk elastic coefficients in the continuum elasticity theory, indicate that a change of the

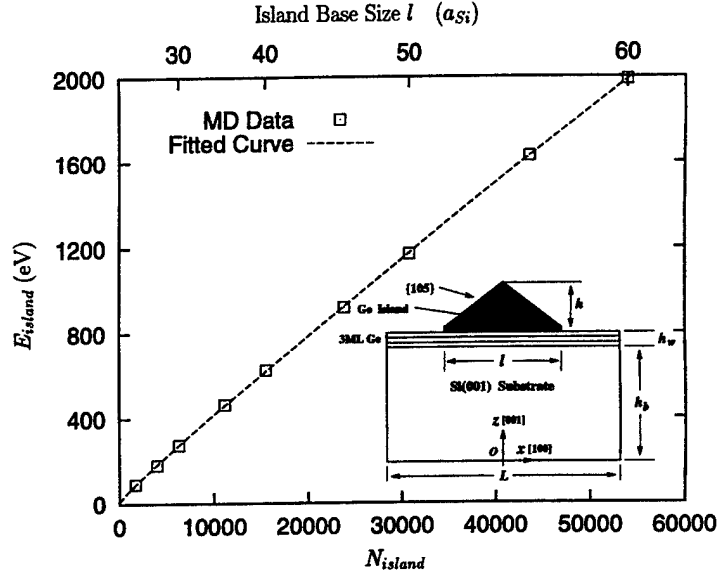


fig. 3

order of 5% to 10% in the elastic coefficients themselves in nanoscale islands can occur. This is a rather significant outcome of these, the first large scale MD studies of the elastic behavior of quantum dots.

In fig. 4 is shown the behavior of the hydrostatic stress ($P_\sigma = (\sigma_{xx} + \sigma_{yy} + \sigma_{zz})/3$) along z for a line passing through the 3D island apex (panel a) and, in panel (b), along x in the topmost Si plane (labeled $N_z=0$) and lowest plane of the Ge island (labeled $N_z=4$, given the 3ML thick WL). In panel (a) are also shown the strain components ϵ_{xx} and ϵ_{zz} . Note the highly inhomogeneous nature of the stress variation, particularly near the edges, through the wetting layer, and the long range of decay into the substrate. Note also in panel (b) the near zero hydrostatic stress at the center of the topmost Si atomic plane ($N_z=0$), becoming increasingly compressive moving towards the island edges. Though not shown here, such a behavior is accompanied by $\sim 0.6\text{\AA}$ upwards vertical displacements of Si atom at the center in the $N_z=0$ atomic plane, decaying monotonically to near zero towards the island edge.

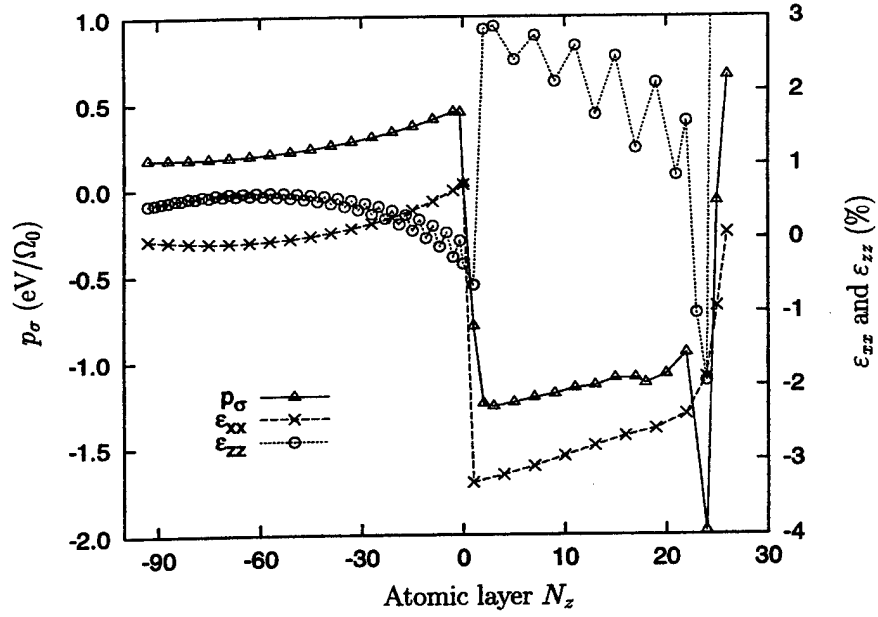


fig. 4.a

The above results (computer experiments) have revealed the true nature of the complex problem of stress and strain distribution on the atomic scale in nanostructures.

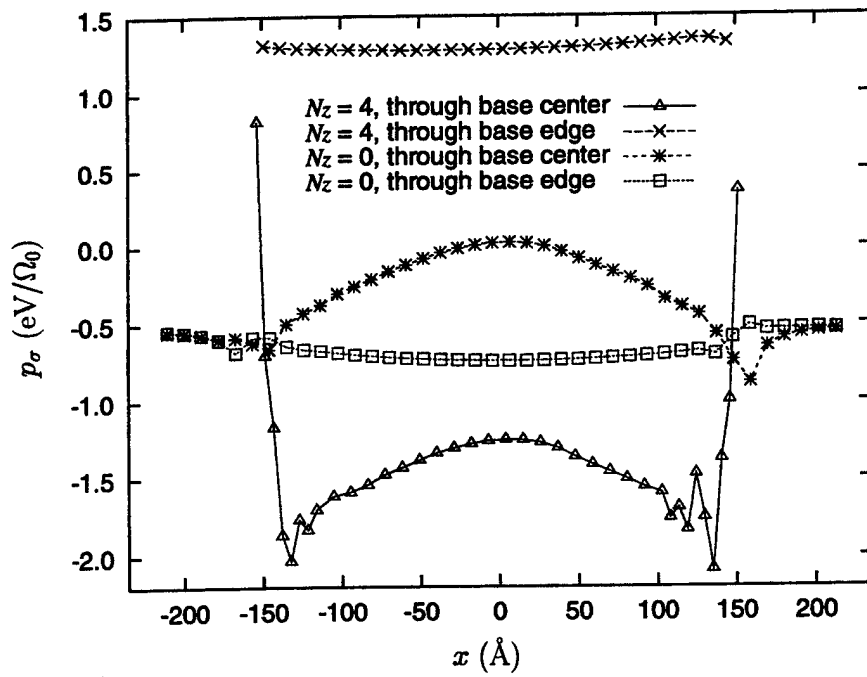


fig. 4.b

They caution us to use judiciously theories that do not account for the discrete nature of solids when the phenomena of significance, such as the initiation and evolution of epitaxial island quantum dots, depend upon the local discrete atomistic kinetic processes.

(d) Island induced stress in capping layer and Vertically Self-Organized quantum dots:

To convert the 3D coherent islands into quantum dots it is necessary to cover the islands with a suitable capping layer without compromising the structural integrity of the islands. Such a capping layer also needs to become planar in its surface morphology within a small thickness beyond the height of the islands. Studies were thus undertaken to elucidate the nature of the cap layer growth by periodically introducing very thin (a few MLs) AlGaAs marker layers during the growth of GaAs cap layer over InAs SAQDs.

Cross-sectional TEM studies revealed evolution of the cap layer profile to be as shown schematically in fig. 5. The stress induced by the lattice mismatch of the GaAs growing on the InAs island sidewalls drives the Ga adatoms away initially before continued arrival of Ga atoms from the vapor planarizes the cap layer surface. This result was demonstrated for the first time in our publication no. 24.

Even after the cap layer morphology has planarized, the buried island induced strain fields persist on the cap layer surface although their strength naturally weakens with increasing thickness of the cap layer. This cap layer surface stress, we argued, can be exploited to grow the next layer of SAQDs in such a way that they predominantly align on top of the dominant islands buried below, thus giving rise to controlled vertical self-organization (VSO) of SAQDs in multiple quantum dot (MQD) structures. Under this grant we carried out,

- (i) molecular dynamics computer simulations of the stress distribution generated by the 3D islands in the cap layer,
- (ii) a simple analytical theory of VSO growth due to stress driven In adatom migration described in terms of surface mechano-chemical potential and continuum elasticity theory, and

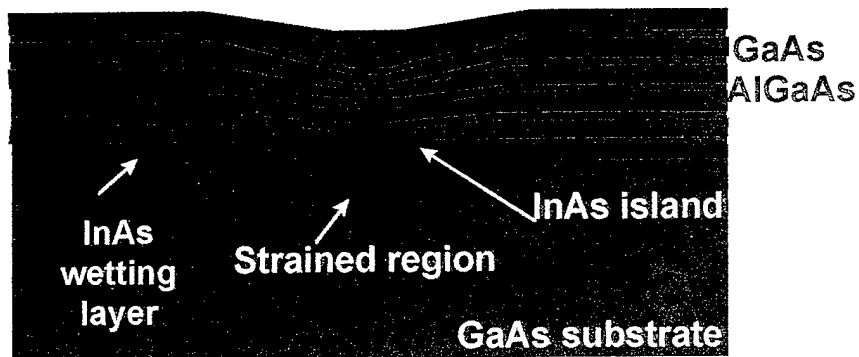


fig. 5

(iii) experimental demonstration of the phenomenon and growth control over vertically self-organized quantum dots. Publication nos. 30, 31, 32 and 36 provide the details. Illustrative results are given below.

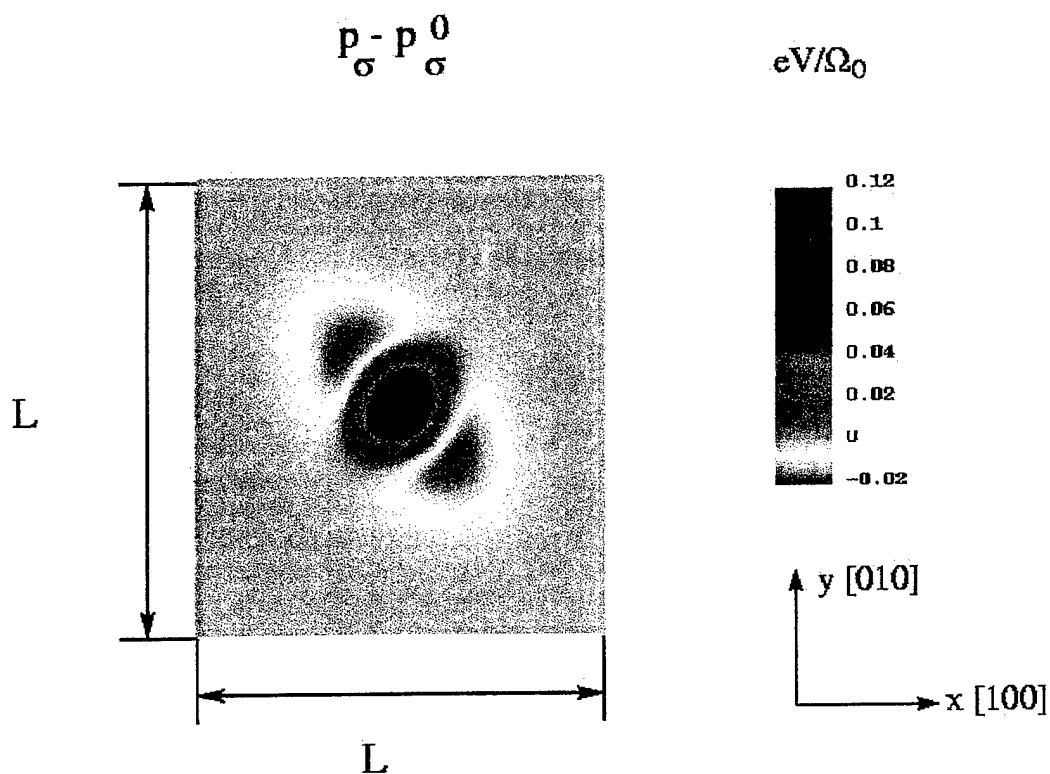


fig. 6

Figure 6 shows a top view of the surface hydrostatic stress distribution on a Si cap layer with a Ge island buried underneath, obtained from our large scale molecular dynamics simulations. The tensile stress above Ge island indicates a dilation of the Si lattice which suggests that upon deposition of Ge, a driving force exists for Ge to preferentially accumulate over such regions of the Si cap layer due to lower strain energy arising from better lattice matching. Details of such stress distributions as a function of the cap layer thickness may be found in publication no. 41.

The presence of such stress-driven adatom migration on spacer layers separating 3D island quantum dot layers can be analytically described in terms of simplified geometrical models of the buried 3D island that provide analytical expressions for the surface stress which, in turn, allow explicit analytical representation of the surface mechano-chemical potential. Combining such surface mechano-chemical potential with a model and analytic expression for atom incorporation at steps/kinks, an expression for the probability of vertical spatial correlation in 3D island positions as a function of relevant geometrical and kinetic parameters can be obtained. Such an analytical description of vertically self-organized growth was provided under this grant for the first time (see publication no. 31). Experiments were carried out for the InAs SAQDs on GaAs(001) and such vertically self-organized stacking in multilayered growth was demonstrated. Figure 7 shows an illustrative cross-sectional TEM image of a stack of five InAs SAQD layers separated by 36ML thick GaAs spacers. Indeed, such structures, developed under this grant, were used as active region of edge-emitting lasers in work supported by AFOSR and ARO and lasing from vertically self-organized SAQDs demonstrated by us for the first time. An illustrative cross-sectional TEM image of such a quantum box laser structure is shown in fig. 8 and its light output versus input current characteristic is shown in fig. 9, indicating onset of lasing at threshold current density of $\sim 310 \text{ A/cm}^2$.

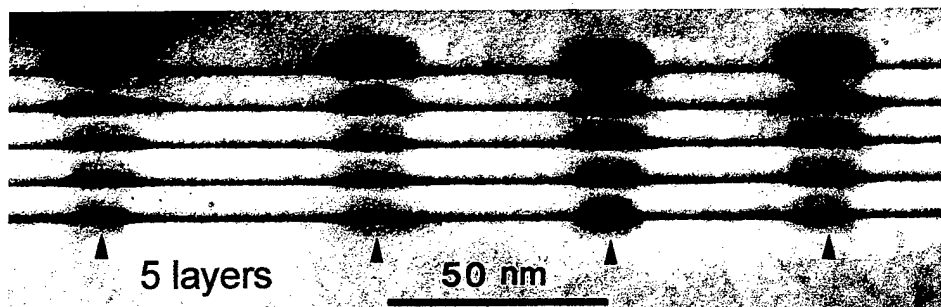


fig. 7

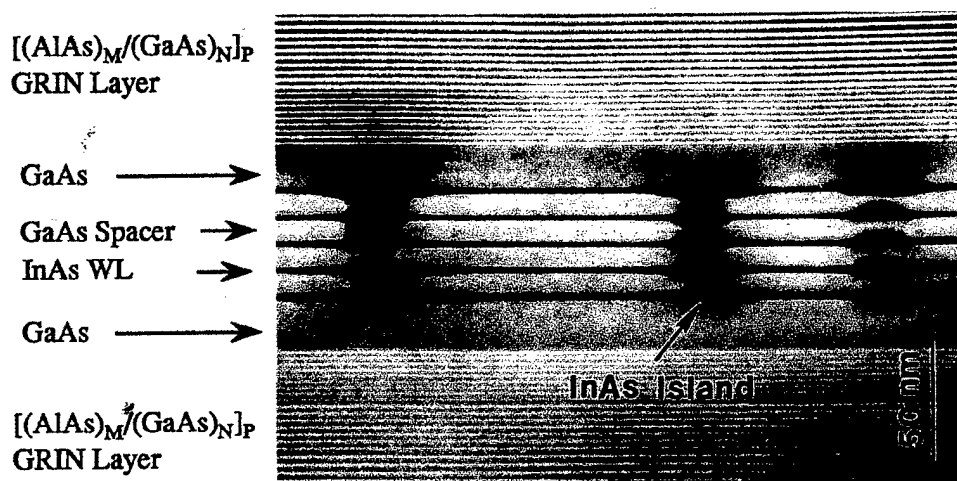


fig. 8

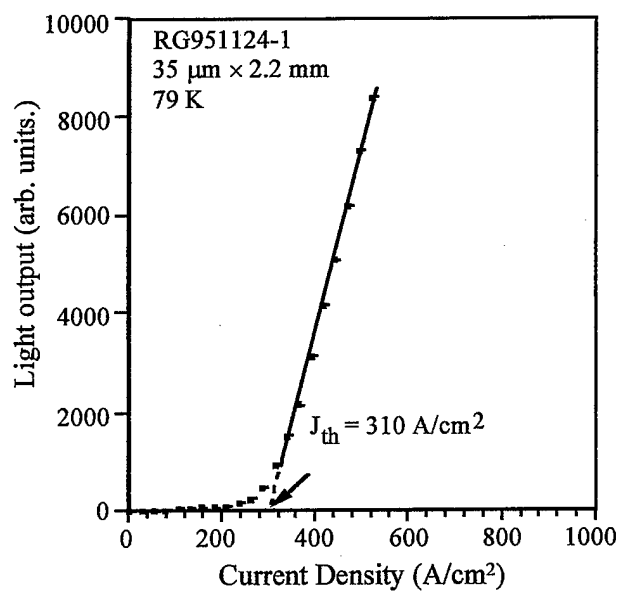


fig. 9

(e) *Independent manipulation of SAQD Density, Size, and Shape: The Variable Deposition Amount (VDA) Structures:*

Under this grant, a major step forward in the control of SAQD density and size was taken through the introduction of the idea of using the first deposited SAQD layer as a seed layer that primarily controls the SAQD density whereas the SAQD size in the subsequent layers is manipulated independently through control of deposition amount and/or composition. In fig. 10 is depicted schematically the idea as implemented by

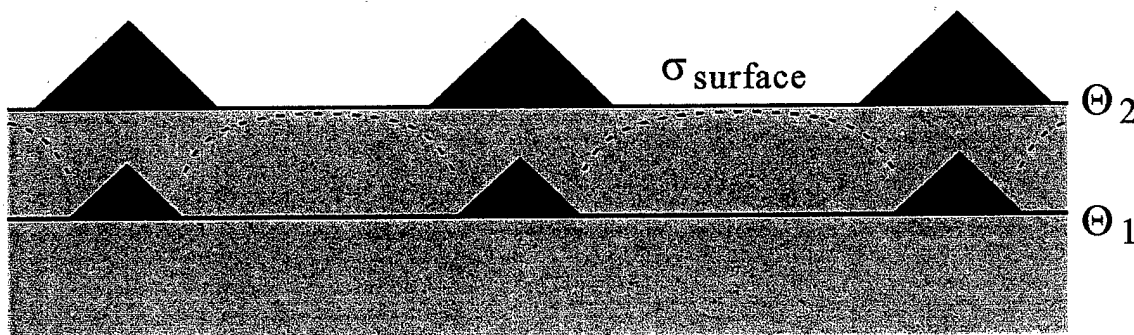


fig. 10

varying the deposition amount of the binary InAs in the seed layer (Θ_1) and the next layer (Θ_2), with $\Theta_2 > \Theta_1$. The amount of additional material ($\Theta_2 - \Theta_1$) in the second layer is guided by our understanding and earlier demonstration (under a preceding ONR contract) of the decreasing growth rate of the strained coherent islands with increasing island size due to an increasing adatom incorporation barrier at island edges. The additional added amount of material is judiciously chosen so as to allow the smaller size islands to catch up, thus increasing the average size and reducing the size nonuniformity. Attendant benefits are longer wavelength operation for lasers and detectors, as well as narrower spectral distribution due to the reduced sensitivity to the same size fluctuations for larger average size, apart from that due to the decrease in size nonuniformity itself.

Details of the growth, AFM characterization of the density, cross-sectional TEM of vertical ordering, and PL and PLE behavior of such structures that we labeled VDA (variable deposition amount) structures are found in publication nos. 51, and 52. In fig. 11 are shown AFM images (inserts) and the height and width distributions of InAs SAQDs for single layer reference samples having deposition amounts 1.74ML and 3ML, and the

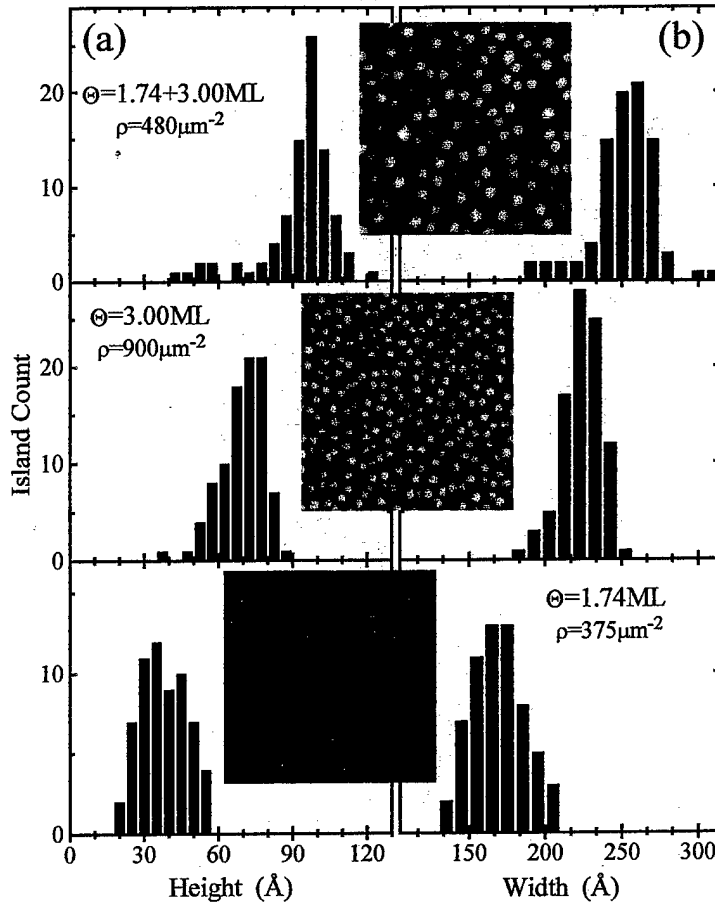


fig. 11

(1.74ML seed + 3.00ML) VDA structure. Note that the SAQD density in the VDA structure is essentially controlled by the seed density but the size has moved independently to larger heights and widths, more so for the height. This suggests a change towards a steeper shape as well for the larger SAQDs. Figure 12 shows the PL behavior of the VDA structures grown with the protective GaAs cap layer. Note the remarkably narrow linewidth of 25meV at 1.028eV ($\sim 1.2\mu\text{m}$) for the (1.74ML + 3.00ML) VDA structure at 6°K. At room temperature, the linewidth is only 29meV and PL emission is at $1.3\mu\text{m}$.

: Excitation Transfer in VDA Structures

The VDA structures developed under this grant allow controlled coupling of vertically-ordered pairs of SAQDs of different size. This opened for the first time a systematic examination of excitation transfer between pairs of vertically coupled SAQDs through varying the thickness and/or composition of the spacer layer. In fig. 13 is shown

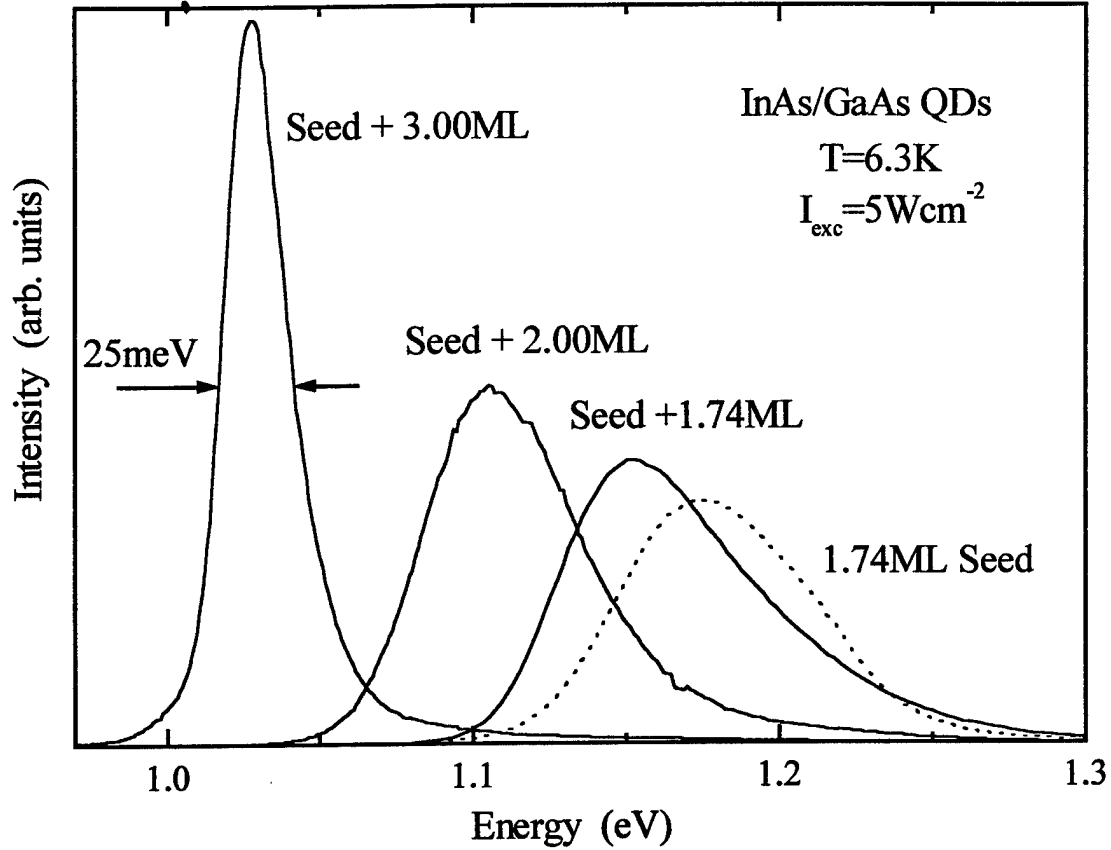


fig. 12

the PL behavior of (1.74ML + 2.00ML) VDA structures with GaAs spacers of thickness 36ML, 45ML, and 54ML (panel a).

In panel (b) is shown the PL from the counterpart structures in which $\text{Al}_{0.2}\text{Ga}_{0.79}\text{As}$ layers of thickness (d_{spacer} - 29ML) have been inserted after 7MLs of GaAs while keeping the total spacer thickness the same as for the three cases in panel (a). The symbol SQD and LQD in fig. 13 denote “small quantum dots” (i.e. the seed layer) and “large quantum dots” (i.e. the next layer). Note the changes in the relative intensity of the small and large QD PL emission manifesting the excitation transfer rate variation arising from changes in the tunneling barrier. From the ratio of the integrated PL intensities of the small and large SAQDs we can extract the excitation transfer yield under the assumption that such transfer is predominantly from the ground state of the smaller SAQDs with a dwell time

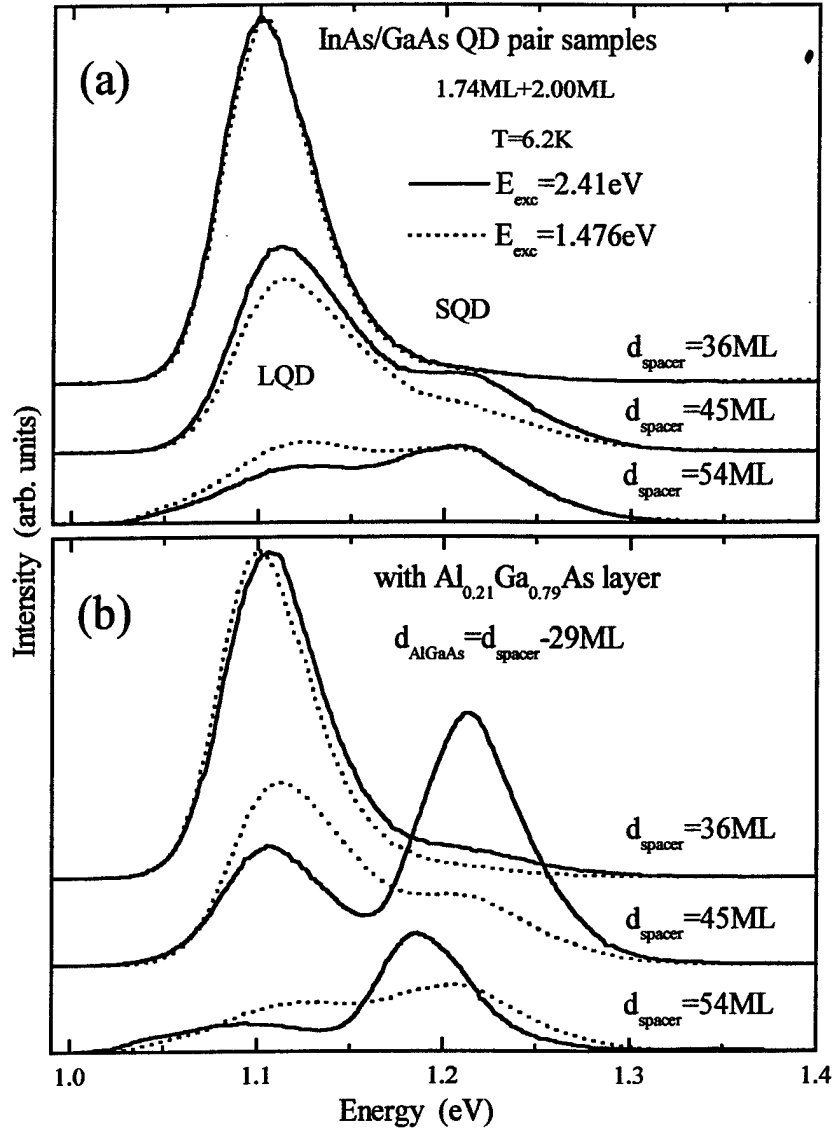


fig. 13

denoted by τ_{dw} . Assuming inter-layer and intra-dot relaxation to be faster than the intra-layer excitation transfer, in this simple model the excitation transfer yield (η_{tr}) is given by,

$$\eta_{tr} = \tau_{SQD} / (\tau_{SQD} + \tau_{dw})$$

in which τ_{SQD} is the ground state lifetime of the small SAQDs. In fig. 14 are shown the behaviors of excitation transfer yield (panel a) and τ_{dw} (panel b) as a function of the spacer thickness. The average tunnel barrier thickness is derived assuming an average height of

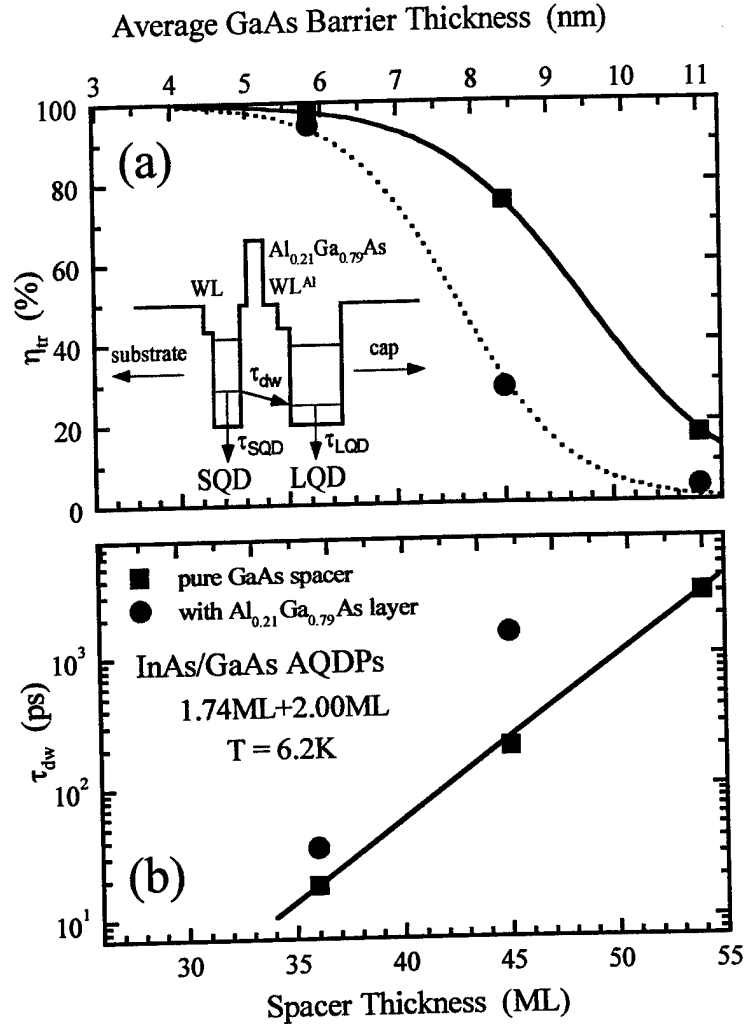


fig.14

4.5nm for the seed (small) quantum dots. Our findings show that the excitation transfer is non-resonant multiphonon-assisted tunneling. Details are found in publication no 52.

II.2. Unstrained and Strained Growth on Patterned Mesas: Size-Reducing Growth, Defect Reduction, and Spatially Selective Quantum Dot Growth.

Work under this grant initiated with studies of MBE growth of lattice matched (GaAs/AlGaAs) and mismatched (GaAs/InGaAs) systems on GaAs(001) substrates patterned with stripe and square mesas. The focus during the period 1991-1994 was on (a) the realization of quantum wires and boxes by purely growth control of the lattice matched GaAs/AlGaAs on appropriately patterned mesas, and (b) on defect reduction in low misfit $In_xGa_{1-x}As$ ($x < 0.2$) thin films via growth on submicron mesas. Subsequently, the efforts

shifted to the growth and characterization of high lattice mismatch InAs on GaAs(001) on nanoscale (c) square and (d) stripe mesas to realize spatially ordered arrays of quantum boxes. Brief summaries of these efforts are provided in subsections (a) through (d) below.

(a) GaAs/AlGaAs Quantum Wires and Boxes via Growth on Mesas:

We examined the nature of GaAs/AlGaAs growth on $[110]$, $[1\bar{1}0]$ and $[100]$ oriented *stripe mesas* on GaAs(001) to shed light on the regime of realization of *quantum wires* on mesa tops. The details of the early work establishing the concept of substrate-encoded size-reducing epitaxy (SESRE) that represents combination of mesa edge orientations and growth conditions that lead to a net migration of adatoms from the mesa sidewalls to the mesa top (and hence reduction in the as-patterned mesa top width, including up to pinch-off, due to growth) are summarized in an overview article, publication no 20.

Utilizing SESRE on $\langle 100 \rangle$ edge oriented *square mesas* on GaAs(001) and on *triangular mesas* provided by the natural 3-fold symmetry of the GaAs(111)B surface, we demonstrated under this grant the very first creation of *quantum boxes* via purely growth control. The specific details are found in the above noted overview article, publication no. 20, and in publication nos. 28, 39 and 42.

The phenomenon of SESRE raises issues concerning the origin of the driving force for inter-facet migration of adatoms between the sidewalls and the mesa top and mesa valley. This remains an unresolved issue to-date although, under this grant, we have speculated and attempted plausible arguments based upon the presence of spatially varying surface stresses inherent to surfaces with patterned profiles. The gradients in the surface stresses, we have postulated, are attendant to the variations in the surface step density (and consequently step-step interactions) when viewed from an atomistic view point that recognizes the discrete nature of the solids. This proposition is reported in publication nos. 18 and 20.

(b) Misfit Dislocation Reduction at low misfits via growth on mesas:

We examined and established defect reduction in low misfit ($<2\%$) lattice mismatched systems, such as $\text{In}_x\text{Ga}_{1-x}\text{As}$ ($x < 0.2$) on $\text{GaAs}(001)$, via growth on mesas of dimensions that render them compliant and hence accommodate, synergistically, a significant amount of the lattice misfit induced strain which on planar substrates is accommodated by the overlayer film through misfit dislocation generation. An enhancement in the critical thickness for the generation of *intrinsic* misfit dislocations was demonstrated for the first time under this grant utilizing the combination of submicron wide stripe mesas on $\text{GaAs}(001)$ and the growth of $\text{In}_x\text{Ga}_{1-x}\text{As}$ ($x < 0.2$). The major findings for the low misfit regime are reported in the overview article, publication no. 20, and in publication nos. 2, 36, and 11. For higher In compositions involving higher lattice mismatch, it was shown that much smaller (i.e. nanoscale) mesas would be required to accommodate the strain. Indeed, examination of this regime of high lattice mismatch and nanoscale mesas has been a major focus of the last renewal period (1995-1999) of this grant. In the following we focus on the findings for the high lattice misfit regime and its connection to the findings noted in Sec. II.1 devoted to the high misfit growth on planar substrates.

: Spatially Selective Quantum Box Growth in highly lattice mismatched systems

We have noted in Sec. II.1 that the growth of highly strained overlayer, such as InAs on $\text{GaAs}(001)$, leads to strain accommodation (at low overlayer thickness) via a change from 2D to 3D coherent island morphology, such 3D islands acting as quantum boxes when appropriately capped. The random spatial location, as well as the inhomogeneity in the volume of these self-assembled quantum dots, are two unsatisfactory features of SAQDs on planar substrates and require improvements to realize their full potential for electronic and opto-electronic devices. To this end, exploring the growth of InAs on nanoscale mesas on $\text{GaAs}(001)$ provided both an opportunity and challenge in the growth - controlled synthesis of regular arrays of uniform sized quantum dots. Under this grant, during 1994-1998, we undertook studies of the growth of InAs on $\text{GaAs}(001)$ square and stripe mesas. In the following we provide a brief summary of the most important findings.

(c) Strain Accommodated Quantum Boxes on Nanoscale Square Mesas:

Nanoscale (<100nm) square mesas were created in-situ via substrate-encoded size-reducing growth (established under this grant as noted in Sec. II.2.a on as-patterned (via ex-situ photolithography) square mesas of linear dimensions $\sim \mu\text{m}$ with their edges along <100> directions. The equivalent nature of all four edges and sidewalls for such mesas allows equivalent size-reducing epitaxy from all four facets and thus in-situ creation of <100nm linear dimension mesas upon which one can deposit the highly lattice mismatched (7%) InAs to create InAs/GaAs quantum boxes (as opposed to the quantum boxes created by depositing GaAs/AlGaAs as described under Sec. II.2.a above). Systematic TEM studies of the behavior of InAs deposition amounts varying from $\sim 3\text{ML}$ up to 24ML on <100nm square mesas were carried out and are detailed in publication nos. 28, 33 and 50. An illustrative behavior is shown in fig. 15.

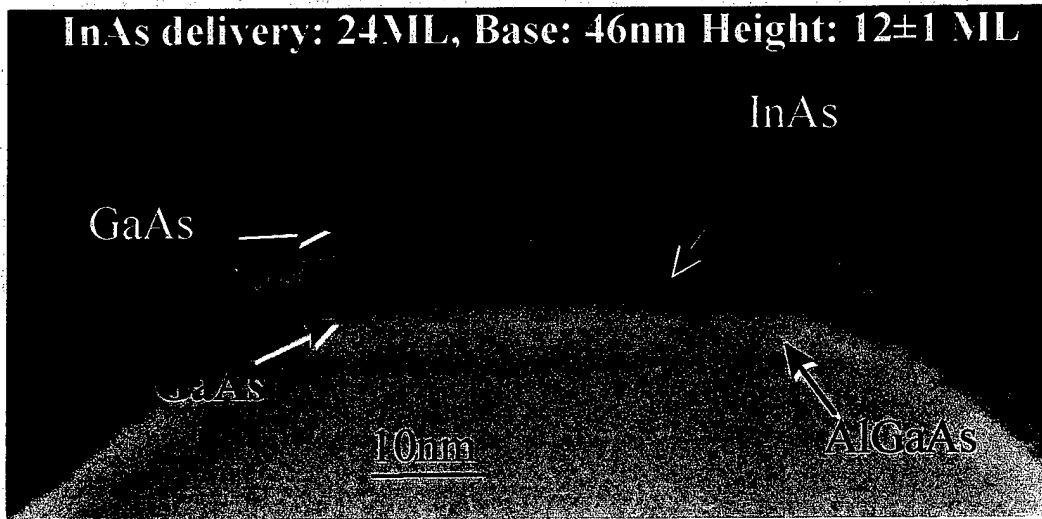


fig. 15

It shows 12ML thick InAs quantum box on a $\sim 46\text{nm}$ base GaAs(001) square mesa. Note that the morphology of the 12ML thick InAs is flat, not the 3D island morphology seen for InAs depositions exceeding $\sim 1.6\text{ML}$ on planar GaAs(001) substrates as discussed in Sec. II.1. This remarkable behavior is due to the compliant nature of the nanoscale GaAs square mesa which accommodates a very large part of the 7% lattice mismatch, thus reducing the strain in the InAs overlayer so much as to allow growth of at least up to 7

times the critical amount without formation of the 3D island morphology. Our studies show that for InAs/GaAs, this behavior occurs for laterally finite mesas of dimensions $<100\text{nm}$. We note also that, at the level of the TEM resolution and statistics, no evidence of the presence of misfit dislocations in such quantum boxes is found.

An equally remarkable phenomena that further manifests the synergistic accommodation of strain/stress with increasing overlayer thickness on nanoscale and its consequences for adatom inter-facet migration is the self-limiting thickness of the overlayer growth shown in fig. 16. Note that the InAs overlayer thickness initially is

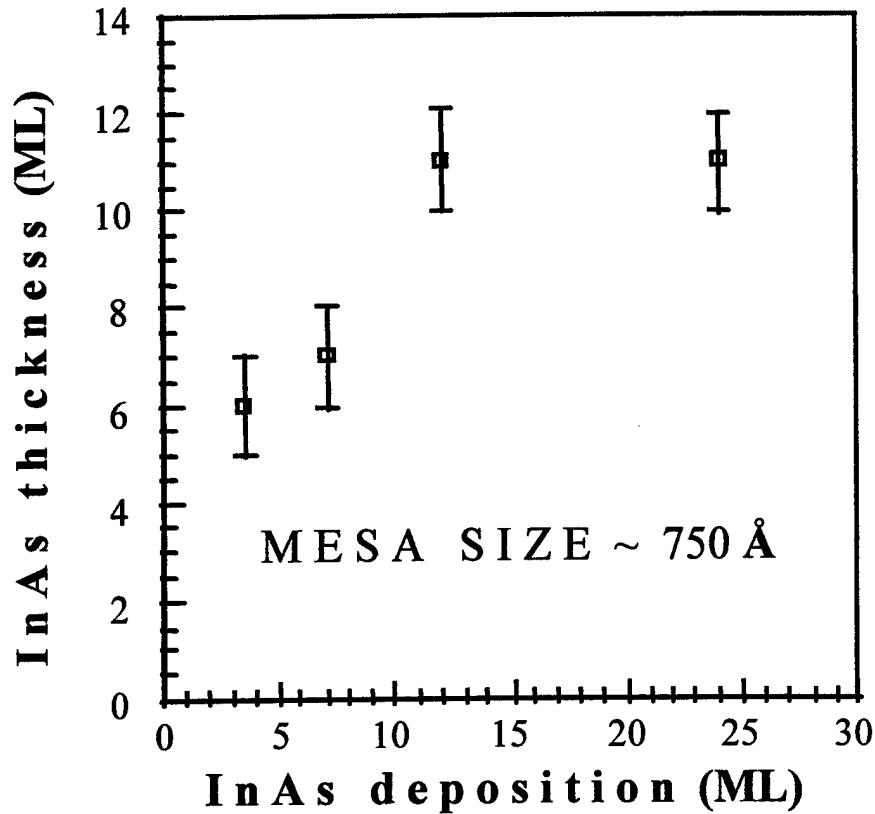


fig. 16

significantly higher than the deposited amount but later is saturated and thus can be significantly less than the deposited amount. This is a consequence of a reversal in the In adatom inter-facet net migration direction due to evolving stress re-distribution and once again brings out the importance of understanding the stress distribution in mesa/overlayer configurations to fully exploit their potential in designing and controlling the growth-controlled synthesis of quantum boxes with optical and electronic properties of potential

use in devices. The optical behavior of such structures was examined by Prof. Daniel Rich and his students, our colleague at USC, utilizing spatially and spectrally-resolved cathodoluminescence studies. The results are reported in publication 28.

: Molecular Dynamics Simulations of Stress Distribution in Overlayer/Nanomesa System

To shed light on the nature of stress distribution in the strained overlayer/nanomesa systems such as the InAs/GaAs combination examined experimentally under this contract, we undertook molecular dynamics simulations utilizing Ge on Si(001) square nanomesas as the vehicle. As also noted in Sec. II.1, this choice is due to the well-tested nature of the available Stillinger-Weber interatomic potentials to model Ge, Si, and their interaction. No comparably reliable potentials for GaAs, InAs, and their interactions

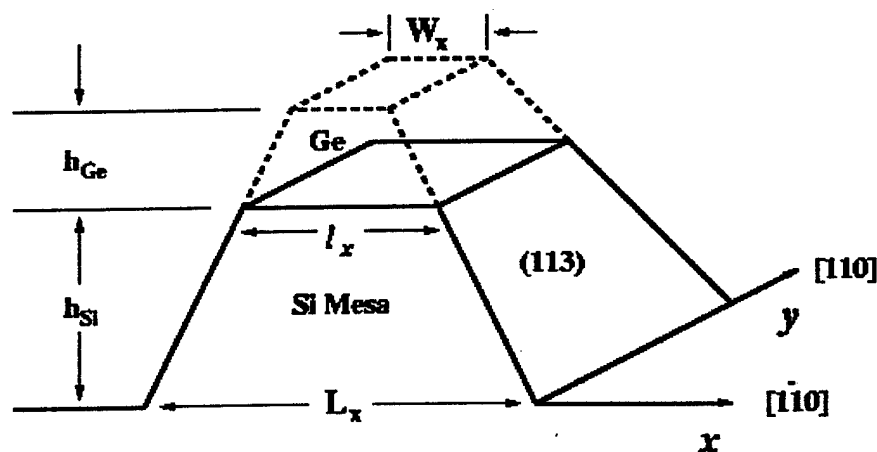


fig. 17

were available in the literature and the scope of this grant did not permit undertaking the development of reliable inter-atomic potentials. It continues to be our hope that such potentials would become available in the near future.

Illustrative results for Ge overlayer on a Si(001) square mesa as schematically depicted in fig. 17 are shown in figures 18 through 21. Figure 18 shows the energy per Ge atom in the structure as a function of Ge overlayer thickness on a Si square mesa of top size 52x52 (in units of Si(001) surface lattice constant) and mesa height of 47ML. Note the sublinear increase in energy (as opposed to the linear increase for thin films on infinite planar substrates) due to the increasing strain accommodation in the compliant Si

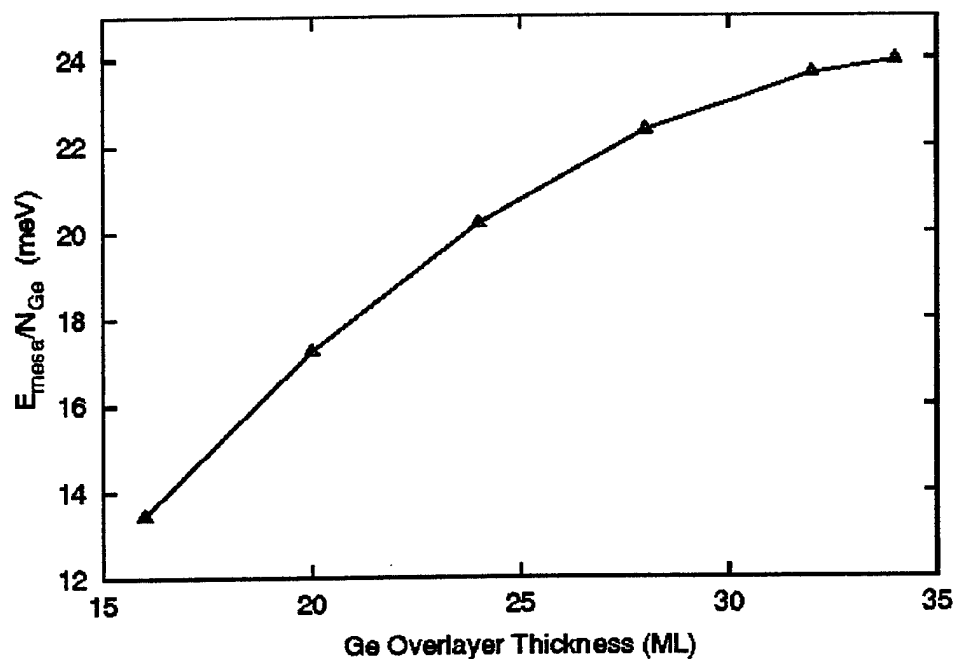


fig. 18

nanoscale mesa. Figure 19 shows the energy per atom for a fixed 16ML thick Ge overlayer on a 52x52 Si(001) square mesa top but with mesa height varying from 7ML to

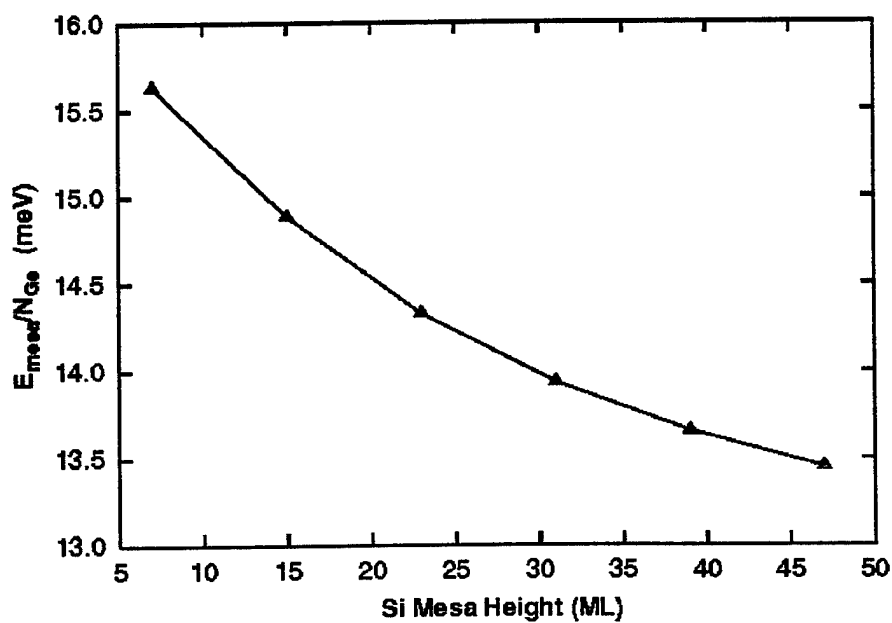


fig. 19

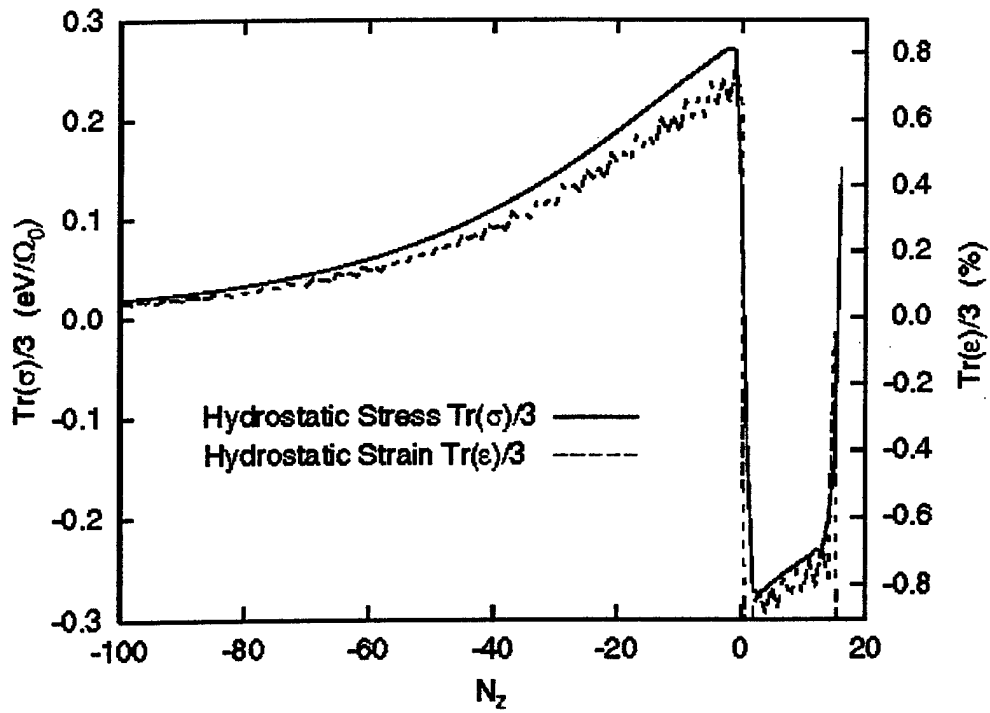


fig. 20

47ML. The decrease in energy observed is a consequence of increasing strain accommodation in the Si nanoscale mesa with increasing height.

In fig. 20 is shown the hydrostatic stress distribution along the center line of the

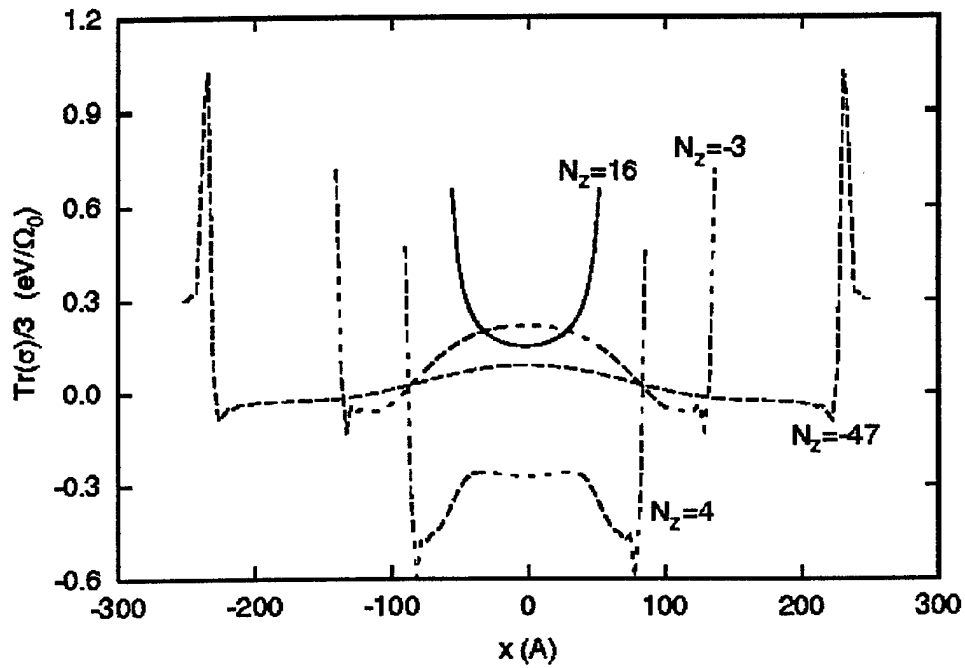


fig. 21

system in the z direction, the depth being denoted by atomic layer number with zero denoting the topmost Si atomic plane of the mesa. Note the nearly 100 atomic layers to which the tensile stress accommodation penetrates into Si (i.e. through the mesa and on into the substrate below). Note also the expected relaxation of the compressive stress in the Ge layer as the distance from the interface increases towards the free surface. Finally, in fig. 21 is shown an illustrative example of the variation of the hydrostatic stress in the x direction along the center lines in the Ge topmost layer ($N_z=16$), fourth Ge layer, the fourth Si layer from the mesa top ($N_z=-3$) and the first continuous Si layer ($N_z=-47$) that defines the first layer of the valleys of the Si substrate. Note that the Ge atom dimerization direction at the surface is in the x direction and is responsible for the tensile strain seen for $N_z=16$ layer. Note the rapid variation in stress at the mesa edges.

(d) Spatially-Selective InAs SAQDs via Growth on Nanoscale Width Stripe Mesas:

As seen above, the growth of InAs on nanoscale laterally finite mesas provides sufficient strain relief in the InAs overlayer as to completely suppress the formation of the strain-driven 3D island morphology-found for planar substrates. If the 3D island based quantum boxes were desired in spatially-selective array, then their growth on nanoscale width stripe mesas may provide a means since strain relief in this case can occur only in one lateral direction. Moreover, exploiting the preferential migration of adatoms from the mesa sidewalls to the mesa top, we can realize InAs 3D island quantum dots on the stripe mesa top for deposition of amount less than the $\sim 1.6\text{ML}$ needed to form islands on infinite planar GaAs(001) surface. This was achieved under this contract and illustrative results are shown in fig. 22 for 1.45ML InAs deposition on in-situ prepared (via SESRE) $[1\bar{1}0]$ stripe mesas of widths 100nm, 60nm, and 30nm. Note the formation of three parallel rows, two parallel rows, and a single row of 3D island quantum dots on stripes of these widths, respectively. The AFM images shown indicate a nominal value of $\sim 30\text{nm}$ as the based width of a typical quantum dot formed under these conditions. This value is limited by the AFM resolution (arising particularly from the tip size convolution effect). Details may be found in publication no. 51.

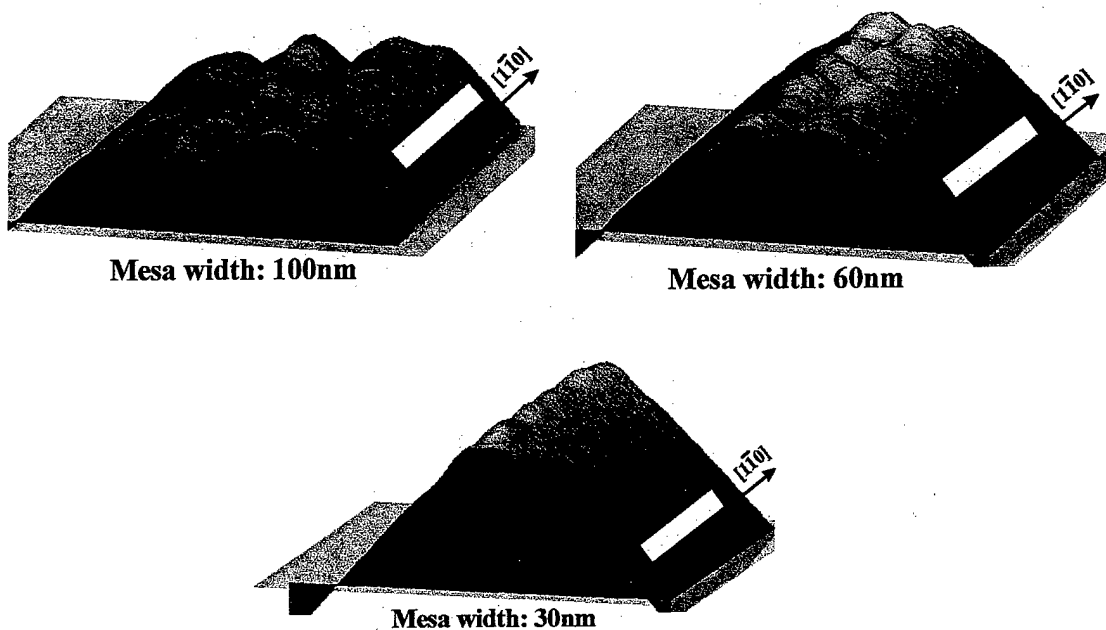


fig. 22

Spatially and spectrally-resolved CL studies were carried out on counterpart samples to the above that have GaAs cap layers. Optically active quantum dots were observed on the mesa tops. Additionally, CL from a low density of quantum dots at the mesa bottom edge with the valley was observed. Quantum dots formed in this region were not detected in the AFM measurements on the uncapped samples, presumably due to spatial resolution limitations. The CL of the SAQDs on the mesa top was found to be red-shifted with respect to that from the SAQDs at the bottom edge. This is indicative of longer average size and/or larger strain relaxation as well in the SAQDs on the mesa top. Polarization dependent CL studies showed a reversal in polarization anisotropy between the CL from the mesa top and bottom edge SAQDs which testifies to the importance of stress anisotropy in both the formation of SAQDs and their optical response. Finally, carrier relaxation kinetics was examined utilizing time-resolved CL studies of such SAQDs for the first time. Details may be found in publication no. 56.

III. List of Publications:

1. S. Guha, K.C. Rajkumar and A. Madhukar, "The Nature and Control of Morphology and the Formation of Defects in InGaAs Epilayers and InAs/GaAs Superlattices Grown via MBE on GaAs(100), Jour. Cryst. Growth, **111**, 434(1991).
2. R. Kapre, A. Madhukar and S. Guha, "Highly Strained Pseudomorphic $\text{In}_x\text{Ga}_{1-x}\text{As}/\text{AlAs}$ Based Resonant Tunneling Diodes Grown on Patterned and Non Patterned GaAs(100) Substrates", Jour. Cryst. Growth, **111**, 1110 (1991).
3. W.C. Tang, H.J. Rosen, S. Guha and A. Madhukar, "Raman Microprobe Study of Narrow $\text{In}_x\text{Ga}_{1-x}\text{As}$ Stripes on Patterned GaAs(100) Substrates", Appl. Phys. Lett. **58**, 1644 (1991).
4. R.M. Kapre, A. Madhukar and S. Guha, "Highly Strained GaAs/InGaAs/AlAs Resonant Tunneling Diodes with Simultaneously High Peak Current Densities and Peak-to-Valley Ratios at Room Temperature", App. Phys. Lett. **58**, 2255 (1991).
5. S.B. Ogale and A. Madhukar, "Surface-Relaxation-Controlled Mechanism for Occurrence of Long Range Ordering in III-V Semiconductor Alloys Grown by Molecular Beam Epitaxy, App. Phys. Lett. **59**, 1356 (1991).
6. Li Chen, KeZhong Hu, K.C. Rajkumar, S. Guha, R. Kapre and A. Madhukar, "Strained InGaAs/GaAs Multiple Quantum Wells Grown on Planar and Pre-Patterned GaAs(100) Substrates Via Molecular Beam Epitaxy: Applications to Light Modulators and Detectors", MRS Proceedings **228**, 213 (1991).
7. K.Z. Hu, L. Chen, R. Kapre, K.C. Rajkumar, A. Madhukar, Z.Karim, C. Kyriakakis and A. Tanguay, Jr., "The Growth and Performance of Strained InGaAs/GaAs Multiple Quantum Well Based Asymmetric Fabry-Perot Reflection Modulators", IEEE/LEOS Topical Meeting on "Epitaxial Materials and in Situ Processing for Optoelectronic Devices", (July 29-31, 1991, Newport Beach, CA) , p.18.
8. S.B. Ogale and A. Madhukar, "Adatom Processes Near Step Edges and Evolution of Long Range Order in Semiconductor Alloys Grown from Vapor Phase", Applied Physics Letters, **60**, 2095 (1992).
9. K.C. Rajkumar, K. Kaviani, J. Chen, P. Chen, and A. Madhukar, "Nanostructures on GaAs(111)B via Photolithography", App. Phys. Letts. **60**, 850 (1992).
10. S. B. Ogale, A. Madhukar, S.Y. Joshi and R. Viswanathan, "Surface Reconstruction, Steps, and Ordering in Semiconductor Alloys Grown from Vapor Phase," J. Vac. Technol. Sci. **10**, 1689 (1992).
11. D. H. Rich, K.C. Rajkumar, Li Chen, A. Madhukar and F.J. Grunthaner, "Defects in Strained $\text{In}_{0.2}\text{Ga}_{0.8}\text{As}/\text{GaAs}$ multiple quantum wells on patterned and unpatterned substrates: A near-infrared cathodoluminescence study," J. Vac. Sci. Technol. **10**, 1965 (1992).
12. D.H. Rich, K.C. Rajkumar, Li Chen, A. Madhukar and F.J. Grunthaner, "Near-infrared cathodoluminescence imaging of defect distributions in $\text{In}_{0.2}\text{Ga}_{0.8}\text{As}/\text{GaAs}$ multiple quantum wells grown on prepatterned GaAs," Appl. Phys. Lett. **61**, 222 (1992).
13. K.C. Rajkumar, K. Kaviani, J. Chen, P. Chen, A. Madhukar, and D.H. Rich, " *In-Situ* approach to realization of three-dimensionally confined structures on patterned GaAs(111)B substrates," MRS Proceed, **263**, 163 (1992).

14. K.C. Rajkumar, K. Kaviani, P. Chen, A. Madhukar, K. Rammohan and D.H. Rich, "One-step *in-situ* quantum dots via molecular beam epitaxy," J. Crystal Growth **127**, 863 (1993).
15. A. Madhukar, K.C. Rajkumar, and P. Chen, "An *in-situ* approach to realization of three-dimensionally confined structures via substrate encoded size reducing epitaxy on nonplanar patterned substrates," Appl. Phys. Lett., **62**, 1547 (1993).
16. W. Chen, P. Chen, R. Viswanathan, A. Madhukar, J. Chen, K. Kaviani, Q. Xie, and K. Hu, "Physical and chemical effects of focused Ga-Ion Beam on GaAs (100)," MRS Symp. Proc. **268**, 301 (1992).
17. W. Chen, P. Chen, A. Madhukar, R. Viswanathan, J. So, "Creation of 3D patterns in Si by focused Ga-Ion beam and anisotropic wet chemical etching," MRS Symp. Proc. **279**, 599 (1993).
18. S. Guha and A. Madhukar, "An explanation for the directionality of interfacet migration during molecular beam epitaxial growth on patterned substrates", J. Appl. Phys. **73**, 8662 (1993).
19. K.C. Rajkumar, A. Madhukar, K. Rammohan, D.H. Rich, P. Chen and L. Chen, "Optically active three-dimensionally confined structures realized via molecular beam epitaxial growth on nonplanar GaAs(111)B", Appl. Phys. Lett. **63**, 2905 (1993).
20. A. Madhukar, "Growth of semiconductor heterostructures on patterned substrates: defect reduction and nanostructure," Thin Solid Films, **231**, 8 (1993).
21. K.C. Rajkumar, A. Madhukar, P. Chen, A. Konkar, L. Chen, K. Rammohan, D.H. Rich, "Realization of Three-Dimensionally Confined Structures via OneStep In-Situ MBE on Appropriately Patterned GaAs (111)," JVST B **12**, 1071 (1994).
22. A. Madhukar, Q. Xie, P. Chen, A. Konkar, "The nature of strained InAs three-dimensional island formation and distribution on GaAs(100)," App. Phys. Lett. **64** 2727 (1994).
23. P. Chen, Q. Xie, A. Madhukar, Li Chen, & A. Konkar, "Mechanisms of Strained Island Formation in Molecular Beam Epitaxy of InAs on GaAs(100)," J. Vac. Sci. Technol. B **12**, 2568 (1994).
24. Q. Xie, P. Chen, and A. Madhukar, "InAs island-induced-strain driven adatom migration during GaAs overlayer growth".App. Phys. Lett. **65**, 2051 (1994).
25. A. Madhukar, "Vapour Phase Synthesis of Thin Films: Towards a Unified Atomistic and Kinetic Framework", Proc. of Symposium, TMS/ASM Mtg., Rosemont, IL, October 2 -6, 1994, Novel Tech. P. 191-210 (1994).
26. Q. Xie, A. Konkar, A. Kalburge, T.R. Ramachandran, P. Chen, R. Cartland, A. Madhukar, H.T. Lin, and D.H. Rich, "Structural and Optical behavior of Strained InAs quantum boxes grown on planar and patterned GaAs(100) Substrates by Molecular beam epitaxy", J. Vac. Sci. Technol. B **13**, 642 (1995).
27. R. Viswanathan, A. Madhukar, and S.B. Ogale, "Role of step orientation and step-step interaction in the *in-situ* creation of laterally confined semiconductor nanostructures via growth: a simulated annealing study on a parallel computing platform", Journal of Crystal Growth **150**, 190 (1995).
28. A. Konkar, K.C. Rajkumar, Q. Xie, P. Chen, A. Madhukar, H.T. Lin, and D.H. Rich, "In-situ fabrication of three-dimensionally confined GaAs and InAs volumes via

- growth on non-planar patterned GaAs(001) substrates", Journal of Crystal Growth **150**, 311 (1995).
29. Q. Xie, P. Chen, A. Kalburge, T.R. Ramachandran, A. Nayfanov, A. Konkar, and A. Madhukar, "Realization of optically active strained InAs island quantum boxes on GaAs(100) via molecular beam epitaxy and the role of island induced strain fields", Journal of Crystal Growth **150**, 357 (1995).
 30. A. Madhukar, P. Chen, Q. Xie, A. Konkar, T.R. Ramachandran, N.P. Kobayashi, and R. Viswanathan, "Semiconductor Nanostructures: Nature's Way", Proc. NATO Advanced Research Workshop, 2/20-24, 1995, Ringberg Castle(Germany), Eds. K. Eberl, P. Demecster, and P. Petroff, Low Dimensional Structures prepared by Epitaxial Growth or Regrowth on Patterned Substrates, (Kluwer Academic Publishers, The Netherlands, 1995), 19-33 (1995).
 31. Q. Xie, A. Madhukar, P. Chen, N. Kobayashi, "Vertically Self-Organized InAs quantum box islands on GaAs(100)", Phys. Rev. Lett. **75**, 2542 (1995).
 32. Q. Xie, N.P. Kobayashi, T.R. Ramachandran, A. Kalburge, P. Chen, and A. Madhukar, "InAs Island Quantum Box Formation and Vertical Self-Organization on GaAs (100) via Molecular Beam Epitaxy", MRS Symp. Proc. Vol. **379**, 177-183 (1995).
 33. A. Konkar, A. Madhukar, and P. Chen, "Creating 3-D Confined Nanoscale Strained Structures Via Substrate Encoded Size-Reducing Epitaxy and The Enhancement of Critical Thickness for Island Formation", Vol. **380**, 17-22 (1995).
 34. A. Madhukar, A. Konkar, and P. Chen, "*In-Situ* Formation of Laterally Confined Semiconductor Structures Via Growth on Nonplanar Patterned Substrates", Paper presented at the Third IU-MRS International Conference(October 17-20, 1995, Seoul, Korea), IUMRS-ICA '95 Proc. (Eds. S.W. Kim and S.J. Park), 1173-1181 (1995).
 35. A. Madhukar, W. Yu, R. Viswanathan, and P. Chen, "Some Computer Simulations of Semiconductor Thin Film Growth and Strain Relaxation in a Unified Atomistic and Kinetic Model", MRS Proc. Vol. **408**, 413 (1995).
 36. Q. Xie, N.P. Kobayashi, T.R. Ramachandran, A. Kalburge, P. Chen, and A. Madhukar, "Strained Coherent InAs Quantum box islands on GaAs(100): Size equalization, vertical self-organization and optical properties", Jour. Vac. Sci. Tech. B **14**, 2203 (1996).
 37. A. Madhukar, "A unified atomistic and kinetic framework for growth front morphology evolution and defect initiation in strained epitaxy", Journal of Crystal Growth **163**, 149 (1996).
 38. R. Heitz, A. Kalburge, Q. Xie, M. Veit, M. Grundmann, P. Chen, A. Madhukar, and D. Bimberg, "Energy relaxation in InAs/GaAs quantum dots", Proc. of the 23rd Int. Conf. on the Physics of Semiconductors, (Berlin Germany, 1996) Editors M. Scheffler and R. Zimmermann, World Scientific, Singapore, 1425 (1996).
 39. P. Chen, A. Konkar, H.T. Lin, D.H. Rich, and A. Madhukar, "Lattice-matched and mismatched quantum boxes fabricated via size-reducing growth on nonplanar patterned substrates", Proc. of the 23rd Int. Conf. on the Physics of Semiconductors, (Berlin, Germany, 1996) Editors M. Scheffler and R. Zimmermann, World Scientific, Singapore, 1277 (1996).

40. W. Yu and A. Madhukar, "Molecular dynamics studies of surface stress in (2 x N) Ge_n/Si(001)", Proc. of the 23rd Int. Conf. on the Physics of Semiconductors, (Berlin, Germany, 1996) Editors M. Scheffler and R. Zimmermann, World Scientific, Singapore, 971 (1996).
41. W. Yu and A. Madhukar, "Molecular dynamics studies of the stress distribution in strained semiconductor nanostructures", Proc. of the 23rd Int. Conf. on the Physics of Semiconductors, (Berlin, Germany, 1996) Editors M. Scheffler and R. Zimmermann, World Scientific, Singapore, 1309 (1996).
42. A. Konkar, H.T. Lin, D.H. Rich, P. Chen, A. Madhukar, "Growth controlled fabrication and cathodoluminescence study of 3D confined GaAs volumes on non-planar patterned GaAs(001) substrates", J. Cryst. Growth **175/176**, 741 (1997).
43. T.R. Ramachandran, R. Heitz, P. Chen, and A. Madhukar, "Mass transfer in Stranski-Krastanow growth of InAs on GaAs", Appl. Phys. Lett. **70**, 640 (1997).
44. R. Heitz, T.R. Ramachandran, A. Kalburge, Q. Xie, I. Mukhametzhanov, P. Chen and A. Madhukar, "Observation of re-entrant 2D to 3D morphology transition in highly strained epitaxy: InAs on GaAs", Phys. Rev. Lett. **78**, 4071 (1997).
45. T.R. Ramachandran, R. Heitz, N.P. Kobayashi, A. Kalburge, W. Yu, P. Chen, and A. Madhukar, "Re-entrant behavior of 2D to 3D morphology change and 3D island lateral size equalization via mass exchange in Stranski-Krastanow growth: InAs on GaAs (001)", J. Cryst. Growth, **175/176**, 216 (1997).
46. A. Kalburge, A. Konkar, T.R. Ramachandran, P. Chen and A. Madhukar, "Focused ion beam assisted chemically etched mesas on GaAs(001) and the nature of subsequent molecular beam epitaxial growth", J. Appl. Phys. **82**, 859 (1997).
47. A. Kalburge, T.R. Ramachandran, R. Heitz, N.P. Kobayashi, Q. Xie, P. Chen, and A. Madhukar, "Optical investigations of InAs growth on GaAs and lasing in singly and multiply stacked island quantum boxes", MRS Proc. Vol. **448**, 487 (1997).
48. T.R. Ramachandran, N.P. Kobayashi, P. Chen, and A. Madhukar, "The formation and evolution of InAs 3D islands on GaAs(001) and a comparative C-AFM and NC-AFM study of InAs 3D islands", MRS Proc. Vol. **440**, 31 (1997).
49. W. Yu and A. Madhukar, "Molecular Dynamics study of coherent island energetics, stresses, and strains in highly strained epitaxy", Phys. Rev. Lett. **79**, 905 (1997), Erratum, **79**, 4939 (1997).
50. A. Madhukar, T.R. Ramachandran, A. Konkar, I. Mukhametzhanov, W. Yu, P. Chen, "On the atomistic and kinetic nature of strained epitaxy and formation of coherent 3D island quantum boxes", Appl. Surface Science, **123/124**, 266 (1998).
51. A. Konkar, A. Madhukar, and P. Chen, "Stress-engineered spatially selective self-assembly of strained InAs quantum dots on nonplanar patterned GaAs(001) substrates", Appl. Phys. Lett. **72**, 220(1998).
52. Y. Tang, D. H. Rich, I. Mukhametzhanov, P. Chen, and A. Madhukar, "Self-assembled InAs/GaAs quantum dots studied with excitation dependent cathodoluminescence", J. Appl. Phys. **84**, 3342(1998).
53. I. Mukhametzhanov, R. Heitz, J. Zeng, P. Chen, and A. Madhukar, "Independent Manipulation of Density and Size of Stress-Driven Self Assembled Quantum Dots", Appl. Phys. Lett. **73**, 1841(1998).

54. R. Heitz, I. Mukhametzhanov, P. Chen, and A. Madhukar, "Excitation Transfer in Self-Organized Asymmetric quantum-dot pairs", Phys. Rev. B **58**, R10151(1998).
55. R. Heitz, M. Veit, A. Kalburge, Q. Xie, M. Grundmann, P.Chen, N.N. Ledentsov, A. Hoffmann, A. Madhukar, D. Bimberg, V. M. Ustinov, P.S. Kop'ev, Zh.I. Alferov, "Hot carrier relaxation in InAs/GaAs quantum dots", Physica E **2**, 578(1998).
56. D. H. Rich, Y. Tang, A. Konkar, P. Chen, and A. Madhukar, "Polarized Cathodoluminescence study of selectively grown self-assembled InAs/GaAs quantum dots", J. App. Phys. **84**, 6337 (1998).

IV. List of Personnel Supported.

Graduate Students:	K. C. Rajkumar,	Ph.D. (1994)
	Q. Xie,	Ph.D. (1996)
	A. Kalburge	Ph.D. (1998)
	A. Konkar	Ph.D. (1999)
	I. Mukhametzhanov	Ph.D. (expected 2000)
Post Doc:	Dr. R. Viswanathan	
	Dr. Wenbin Yu	
P.I.:	Prof. A. Madhukar	